Neuron, Vol. 48, 605–618, November 23, 2005, Copyright ©2005 by Elsevier Inc. DOI 10.1016/j.neuron.2005.09.027

Activity-Dependent Dendritic Spine Structural Plasticity Is Regulated by Small GTPase Rap1 and Its Target AF-6

Zhong Xie,[1] Richard L. Huganir,[2] and Peter Penzes[1,*]
[1] Department of Physiology
Northwestern University Feinberg
School of Medicine
303 East Chicago Avenue
Chicago, Illinois 60611
[2] Department of Neuroscience
and Howard Hughes Medical Institute
The Johns Hopkins University School of Medicine
725 North Wolfe Street
Baltimore, Maryland 21205

Summary

Activity-dependent remodeling of dendritic spines is essential for neural circuit development and synaptic plasticity, but the mechanisms that coordinate synaptic structural and functional plasticity are not well understood. Here we investigate the signaling pathways that enable excitatory synapses to undergo activity-dependent structural modifications. We report that activation of NMDA receptors in cultured cortical neurons induces spine morphogenesis and activation of the small GTPase Rap1. Rap1 bimodally regulates spine morphology: activated Rap1 recruits the PDZ domain-containing protein AF-6 to the plasma membrane and induces spine neck elongation, while inactive Rap1 dissociates AF-6 from the membrane and induces spine enlargement. Rap1 also regulates spine content of AMPA receptors: thin spines induced by Rap1 activation have reduced GluR1-containing AMPA receptor content, while large spines induced by Rap1 inactivation are rich in AMPA receptors. These results identify a signaling pathway that regulates activity-dependent synaptic structural plasticity and coordinates it with functional plasticity.

Introduction

Dendritic spine morphogenesis plays a central role in brain development and plasticity (Hering and Sheng, 2001; Yuste and Bonhoeffer, 2001). During development, activity-dependent structural plasticity of dendrites and synapses is essential for the formation and refinement of neuronal circuits (Lendvai et al., 2000; Wong et al., 2000; Wong and Wong, 2000; Yuste and Bonhoeffer., 2001). This is well exemplified by the massive spine turnover during the critical period in the barrel and visual cortices and its regulation by experiences such as whisker trimming or monocular deprivation (Lendvai et al., 2000; Mataga et al., 2004; Oray et al., 2004). In mature animals, activity-dependent changes of the postsynaptic structure are thought to contribute to the plasticity of neural circuits and possibly to learning and memory (Yuste and Bonhoeffer, 2001). For example, modulation of sensory experience in live animals, such as whisker trimming, results in increased spine turnover in the barrel cortex, and these changes contribute to circuit refinement (Trachtenberg et al., 2002; Holtmaat et al., 2005). At the cellular level, induction of long-lasting potentiation of CA1 synapses by high-frequency stimulation results in the input-specific appearance of new spines or remodeling of the existing spines (Engert and Bonhoeffer, 1999; Maletic-Savatic et al., 1999; Toni et al., 1999; Nagerl et al., 2004). Such structural changes are thought to complement functional changes in synaptic strength (Malenka and Nicoll, 1999) and provide neural circuits the ability to rewire (Chklovskii et al., 2004). In addition, many neurodevelopmental and neuropsychiatric disorders are associated with defects in dendritic spine morphology and activity-dependent structural plasticity (Fiala et al., 2002; Halpain et al., 2005).

Several studies have implicated NMDA receptors and CaMKII in regulating activity-dependent structural plasticity (Maletic-Savatic et al., 1999; Toni et al., 1999; Wu et al., 2001; Jourdain et al., 2003). However, the molecular details of the intracellular signal transduction mechanisms regulating structural plasticity are largely unknown. Because structural and functional plasticity appear to be coordinated, it is particularly important to identify and characterize the common regulators of functional and structural plasticity that may coordinate these two aspects of synaptic plasticity (Luscher et al., 2000; Kasai et al., 2003).

Synaptic signal transduction molecules play a critical role in regulating and coordinating different aspects of synaptic plasticity (Sheng and Kim, 2002; Kasai et al., 2003). One such signaling molecule is the Ras-like small GTPase Rap1, a regulator of multiple cellular events, including adhesion, cell polarity, and proliferation (Caron, 2003; Stork, 2003). Recent work implicated Rap1 in the regulation of AMPA receptor synaptic endocytosis during LTD (Zhu et al., 2002; Imamura et al., 2003), in dendritic development (Chen et al., 2005), and in regulation of neuronal excitability, synaptic plasticity, learning, and memory (Morozov et al., 2003). In addition, a RapGAP, SPAR, regulates dendritic spine morphology (Pak et al., 2001). Therefore, Rap1 may be a key regulator of activity-dependent and -independent spine morphogenesis and a coordinator of functional and structural plasticity.

Little is known about the targets of Rap1 or, in particular, about those that may have synaptic functions (Hering and Sheng, 2001). One of the few known Rap1-binding proteins is AF-6, a protein associated with epithelial adhesion junctions (Kuriyama et al., 1996; Mandai et al., 1997). AF-6 binds activated Rap1 with a higher affinity than Ras or Rap2 (Linnemann et al., 1999; Boettner et al., 2000), and in *Drospohila* the AF-6 homolog *canoe* functions as a Rap1 effector (Boettner et al., 2003), suggesting that Rap1 may be an in vivo AF-6 target. Two splice variants of AF-6 are expressed in the brain, a short (170 kDa) and a long isoform (205 kDa) (Mandai et al., 1997). L-AF-6 has two Ras/Rap-binding (RA) motifs, a kinesin-like and a myosin-like domain, followed by a

*Correspondence: p-penzes@northwestern.edu

PDZ domain. At the C terminus, L-AF-6 has a filamentous actin-binding domain. AF-6 has been previously shown to localize to synapses (Buchert et al., 1999; Nishioka et al., 2000). Therefore, AF-6 is a strong candidate to mediate Rap1 effects on spine morphogenesis.

In this study, we investigated the intracellular signaling pathways that confer neurons the ability to alter their dendritic and synaptic morphology in response to changes in synaptic activity. We report that activation of NMDA receptors in neuronal cultures induces dramatic spine morphogenesis. We show that Rap1, which is activated after NMDA receptor activation, regulates synaptic structural plasticity in a bimodal fashion. We identify AF-6 as a postsynaptic target of activated Rap1 and show that Rap1 regulates the membrane recruitment of AF-6. AF-6 regulates spine morphogenesis in a similar manner as NMDA receptor activation and activated Rap1. In addition, Rap1 regulates AMPA receptor content in spines. Altogether, we provide evidence that Rap1 and AF-6 function in a postsynaptic signaling pathway that regulates synaptic structural changes during synaptic plasticity.

Results

NMDA Receptor Activation Induces Spine Morphogenesis

Recent studies suggested that patterned synaptic activity induces dendritic spine morphogenesis in experimental systems such as brain slices and in intact animals (Engert and Bonhoeffer, 1999; Maletic-Savatic et al., 1999; Toni et al., 1999; Trachtenberg et al., 2002; Holtmaat et al., 2005; Oray et al., 2004). Activation of NMDA receptors is essential for the induction of activity-dependent structural plasticity of spines in hippocampal dissociated neuronal and slice cultures (Maletic-Savatic et al., 1999; Toni et al., 1999; Wu et al., 2001). To investigate the intracellular mechanisms of activity-dependent structural plasticity of synapses, we set out to identify and characterize the mechanisms and signal transduction pathways that link NMDA receptor activation with structural plasticity of spines. We therefore sought to find a method to induce spine formation by activation of NMDA receptors with stimuli that also induced activity-dependent functional plasticity in cultured neurons. We used primary cultures of cortical neurons to allow for a better visualization of morphological events and as a model system to study the underlying intracellular signaling mechanisms. Previous studies have shown that activation of NMDA receptors by withdrawal of the NMDA receptor antagonist APV from neurons cultured in APV resulted in insertion of AMPA receptors into silent synapses and induction of potentiation of the mEPSCs (Liao et al., 1999, 2001; Lin et al., 2004). We wanted to determine whether this treatment also induced spine morphogenesis. To visualize the morphology of spines, neurons were transfected with GFP and then subjected to APV withdrawal (APV wd). Control neurons were maintained in APV (+APV). We observed that removal of APV for 30 min from 4-week-old cortical neurons cultured in presence of 200 μM APV, followed by a recovery of 2 hr in APV-containing medium, resulted in dramatic spine morphogenesis. This structural plasticity appeared as an increase in the number of thin and long spines with elongated necks and an overall increase in the number of dendritic protrusions (Figure 1A-B). Double staining of these cultures with an antibody against the presynaptic marker bassoon revealed that the majority of these elongated spines contacted presynaptic terminals, suggesting that they may be functional spines (Figure 1C). We used single-factor ANOVA analysis to quantify this and all other data sets and to determine the statistical significance of the differences between experimental groups (Penzes et al., 2003). In treated neurons (APV wd) versus control (+APV) neurons, the averages of spine areas ($1.33 \pm 1.0\ \mu m^2$ versus $0.50 \pm 0.3\ \mu m^2$, ANOVA: $p < 0.0001$), length ($2.81 \pm 1.53\ \mu m$ versus $1.16 \pm 0.75\ \mu m$, $p < 0.0001$), and density (44.5 ± 4.5 spines/100 μm versus 29.1 ± 4.2 spines/100 μm, $p < 0.0001$) were significantly different (Figure 1D).

Rap1 Is Regulated by Synaptic Activity

We next sought to identify signaling mechanisms that mediated spine morphogenesis induced by NMDA receptor activation upon APV withdrawal. Because the small GTPase Rap1 has recently been implicated in the regulation of dendritic development, AMPA receptor trafficking during synaptic plasticity, neuronal excitability, and learning and memory, it was likely that it was also important for structural plasticity (Zhu et al., 2002; Morozov et al., 2003, Imamura et al., 2003; Chen et al., 2005). To determine whether Rap1 was activated following NMDA receptor activation in 4-week-old dissociated primary cortical neuronal cultures, we activated NMDA receptors by APV withdrawal, and 2 hr later we examined the activation of endogenous Rap1 using an affinity binding-based activity assay (Rebhun et al., 2000). Western blotting revealed that while there was a low level of basal Rap1 activation, APV withdrawal resulted in a significant enhancement in Rap1 activation (statistically significant difference by Student's t test, $p < 0.01$) (Figures 1E and 1G). To determine whether another chemical treatment known to induce plasticity-like phenomena in cultured neurons also regulated Rap1 activation, we treated cortical neurons cultured in the absence of APV with 100 μM glycine for 3 min (Figures 1F and 1G; $^*p < 0.05$) (Lu et al., 2001). This treatment is thought to activate exclusively synaptic NMDA receptors and results in an increase in mEPSC frequency and amplitude. In accordance with the previous experiment, treatment with glycine also resulted in activation of Rap1. These experiments demonstrate that activation of NMDA receptors by stimuli that also induce functional plasticity-like events results in activation of Rap1, suggesting that Rap1 may be a mediator of NMDA receptor activation-dependent spine structural plasticity.

Rap1 Regulates Dendritic Spine Morphogenesis

Rap1 is present in the PSD (Mizoguchi et al., 1990), and a regulator of Rap, the Rap-GAP SPAR, has been shown to induce changes in spine morphology, suggesting that Rap signaling may regulate spine morphogenesis (Pak et al., 2001). Therefore, we reasoned that Rap1 may also play a key role in regulating synaptic structural plasticity. To examine the function of Rap1 in regulating spine morphogenesis, we transfected cortical neuronal cultures (DIV 21) with constitutively active Rap1-63E

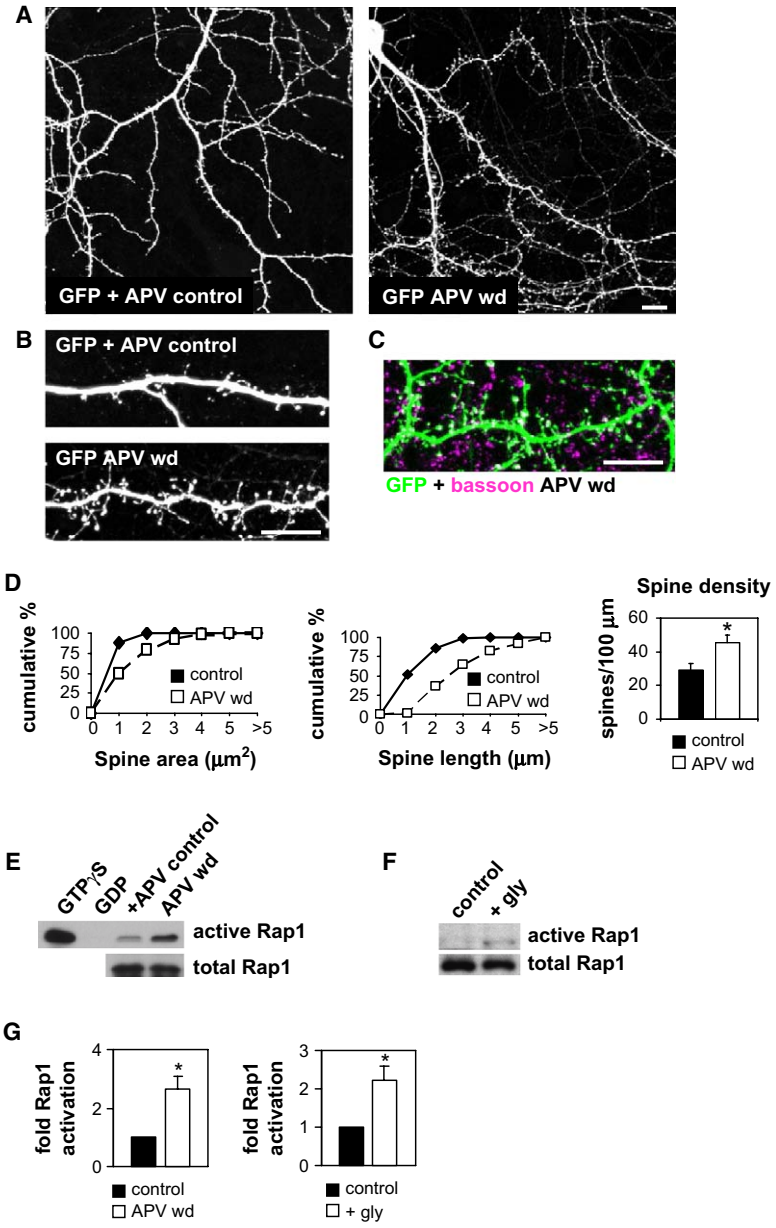

Figure 1. NMDA Receptor-Dependent Spine Morphogenesis and Rap1 Activation

Activation of NMDA receptors induces spine morphogenesis and activates Rap1 in cultured cortical pyramidal neurons. (A) Activation of NMDA receptors by withdrawal of APV (in the presence of 10 μM glycine) for 30 min from cortical neurons (DIV 28) cultured in the presence of D,L-APV (200 μM) induces elongation of spines and an increase in spine density. (B) Higher-magnification images of control and treated neurons. (C) Spines induced by NMDA receptor activation contact presynaptic terminals, as revealed by immunofluorescence staining with an antibody for the presynaptic protein bassoon. (D) Quantification of the effects of APV withdrawal on spine morphogenesis. The averages of spine areas (1.33 ± 1.0 μm^2 versus 0.50 ± 0.3 μm^2, ANOVA: $p < 0.0001$), length (2.81 ± 1.53 μm versus. 1.16 ± 0.75 μm, $p < 0.0001$), and density (44.5 ± 4.5 spines/100 μm versus 29.1 ± 4.2 spines/100 μm, $p < 0.0001$) were significantly different. (E) Rap1 is activated upon APV withdrawal from cortical neurons (DIV 28) cultured in the presence of APV (200 μM). Rap1 activity was determined with an affinity-isolation-based activity assay. Resin-bound GTP-Rap1 was detected by Western blotting with a polyclonal antibody for Rap1. (F) In neurons cultured without APV, activation of synaptic NMDA receptors by the addition of glycine (100 μM) for 3 min activates Rap1. (G) Quantification of Rap1 activation by APV withdrawal (left) and glycine treatment (right). Plots are averages of Rap1 activation from three experiments. Values for Rap1 activation were normalized to the expression levels of Rap1 protein. The differences between APV withdrawal versus control (*$p < 0.01$) and glycine treatment versus control (*$p < 0.05$) were statistically significant (Student's t test). Scale bars, 10 μm. Bars represent averages of data from three experiments; error bars are standard deviations.

(Rap1-CA) or RapGAP1 to inactivate Rap, along with GFP (Figure 2) (Rubinfeld et al., 1991). Two days later (at DIV 23), we fixed and stained the neurons. In transfected neurons, Rap1-CA was in the soma and dendritic shafts, but it was also present in the spine heads of a considerable fraction of spines, suggesting that it may be partially targeted to spines (arrowheads) (Figure 2A).

Neurons expressing Rap-CA had significantly longer spines compared to neurons expressing GFP alone (Figure 2A, arrowheads): length (2.82 ± 1.6 μm versus 1.24 ± 0.5 μm, $p < 0.0001$); area (1.25 ± 1.08 μm^2 versus 0.47 ± 0.29 μm^2, $p < 0.0001$) (Figure 2B). However, the spine densities were similar between the control and Rap-CA-expressing neurons (31.77 ± 5.4 spines/100 μm versus 28.7 ± 4.0 spines/100 μm, $p = 0.2$). An intriguing feature of these spines was that they were thin and long and closely resembled those induced by APV withdrawal. In contrast, in neurons expressing RapGAP1, we observed an increase in spine sizes that resulted in increased average spine area compared to those on control or Rap1-CA-expressing neurons (RapGAP1: area, 1.97 ± 1.1 versus 0.47 ± 0.29, $p < 0.0001$; length, 1.74 ± 1.0 versus 1.25 ± 0.5, $p < 0.0001$) (Figure 2A, open arrowheads). Expression of Rap1-CA or RapGAP1 had no effect on spine density. Statistical analysis revealed that the spine elongation morphologies induced by APV withdrawal and Rap1 activation were similar and statistically indistinguishable (area, 1.33 ± 1.0 μm^2 versus 1.25 ± 1.08 μm^2, $p = 0.75$; length, 2.81 ± 1.53 μm versus 2.82 ± 1.6 μm, $p = 0.37$), suggesting that Rap1 may link synaptic NMDA receptor activation to spine morphogenesis.

AF-6 Is a Synaptic Target of Rap1

Because we have shown that Rap1 regulates spine morphogenesis, we became interested in identifying Rap1

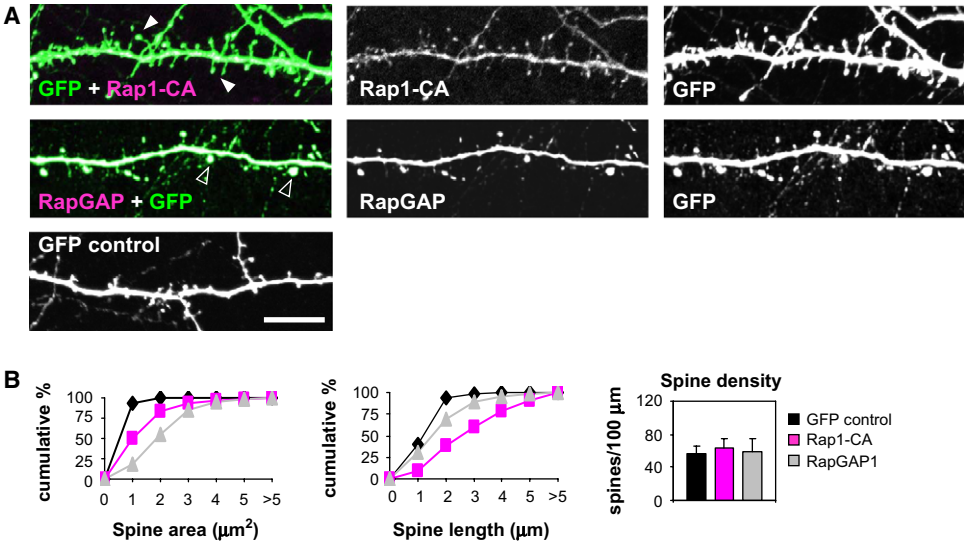

Figure 2. Rap1 Regulates Spine Morphogenesis

(A) Overexpression of constitutively active Rap1-63E (Rap1-CA) in cortical neurons induces spine elongation (arrowheads), while inactivation of Rap1 by overexpressing dominant-negative Rap1-17N (Rap1-DN) or RapGAP1 induces spine enlargement (open arrowheads). High-density cultures of cortical neurons (DIV 21) were transfected with GFP alone or with HA-Rap1-CA, *myc*-Rap1-DN, or flag-RapGAP1 and 40 hr later were fixed and stained. GFP was detected using an anti-GFP antibody; the other exogenous proteins were detected using antibodies against their tags. (B) Quantification of the effects of Rap1 mutants on spine area, length, and density. Rap-CA versus control: length (2.82 ± 1.6 μm versus 1.24 ± 0.5 μm, $p < 0.0001$); area (1.25 ± 1.08 μm^2 versus 0.47 ± 0.29 μm^2, $p < 0.0001$); density (31.77 ± 5.4 spines/100 μm versus 28.7 ± 4.0 spines/100 μm, $p = 0.2$). RapGAP1 versus control: area (1.97 ± 1.1 μm^2 versus 0.47 ± 0.29 μm^2, $p < 0.0001$); length (1.74 ± 1.0 μm versus 1.25 ± 0.5 μm, $p < 0.0001$). Scale bar, 10 μm. Bars represent averages of data from three experiments; error bars are standard deviations.

targets that may mediate its function in structural plasticity. Little is known about direct binding targets of activated Rap1 in general and in synapses in particular. We therefore searched for proteins that contained Rap1-binding motifs and that could potentially be localized to synapses. One such protein was AF-6, previously characterized as a component of epithelial adherens junctions (Kuriyama et al., 1996; Mandai et al., 1997; Boettner et al., 2000). AF-6 has been reported to interact with both Rap and Ras; however, it binds Rap1 with a much higher affinity that Ras or Rap2, suggesting that Rap1 rather than Rap2 or Ras may be the physiological regulator of AF-6 (Linnemann et al., 1999; Boettner et al., 2000). In addition, AF-6 has been previously shown to be localized to synapses by electron microscopy and immunohistochemistry (Buchert et al., 1999; Nishioka et al., 2000). Moreover, AF-6 interacted in a yeast two-hybrid screen with the C terminus of the Rac1 GEF kalirin-7, a key regulator of spine morphogenesis (Penzes et al., 2001). Therefore, AF-6 may be a postsynaptic Rap1 target in regulating structural plasticity.

To test this hypothesis, we examined the synaptic localization of AF-6 by subcellular fractionation and immunocytochemistry and analyzed the functional coupling of Rap1 to AF-6 in neurons. To examine more thoroughly the synaptic localization of AF-6, we performed subcellular fractionation of rat cerebral cortex and immunocytochemistry of dissociated cultures of hippocampal neurons (Figure 3A). In subcellular fractions of rat cerebral cortex, both forms of AF-6 were roughly equally distributed between the soluble (S1) and particulate (P1) fractions, suggesting that in brain there are pools of soluble as well as membrane/cytoskeleton-associated AF-6 (Figure 3A). Detergent extraction of the synaptosomal fraction, a method designed to detect proteins enriched in the postsynaptic density, revealed that both isoforms of AF-6 were highly enriched in the postsynaptic density (PSD) fractions (Figure 3A). Moreover, by immunostaining mature hippocampal neurons (DIV 24) with the use of an antibody that recognizes both forms of AF-6 we found that, while AF-6 was present in the dendritic shaft, it was concentrated in spine-like structures and partially colocalized with the presynaptic marker bassoon as well as with the AMPA-type glutamate receptor subunit GluR2, a marker for excitatory synapses (Figure 3B, arrowheads). In conclusion, AF-6 is a protein concentrated in a subset of excitatory synapses.

Rap1 Regulates the Subcellular Localization of AF-6

Activated GTP-bound Rap1 binds to AF-6 with much higher affinity than its inactive GDP-bound form (Linnemann et al., 1999; Boettner et al., 2000). Therefore, we reasoned that Rap1, depending on its state of activation, may regulate AF-6 localization or function. We initially examined this possibility using hEK293 cells (Figure 4A). When expressed alone in these cells, AF-6 was both cytosolic and membrane associated, as shown by immunostaining, while Rap1-CA was concentrated in patches at the plasma membrane (arrowheads). To examine the effect of Rap1 activation or inactivation on AF-6 localization, we overexpressed AF-6 together with Rap1-CA or RapGAP. In cells coexpressing Rap1-CA, AF-6 was significantly more membrane localized and colocalized with exogenous Rap1-CA in punctate structures at the plasma membrane (arrowheads). In contrast, when coexpressed with RapGAP, all the AF-6 protein was completely soluble, with very little associated with the plasma membrane. Hence, Rap1

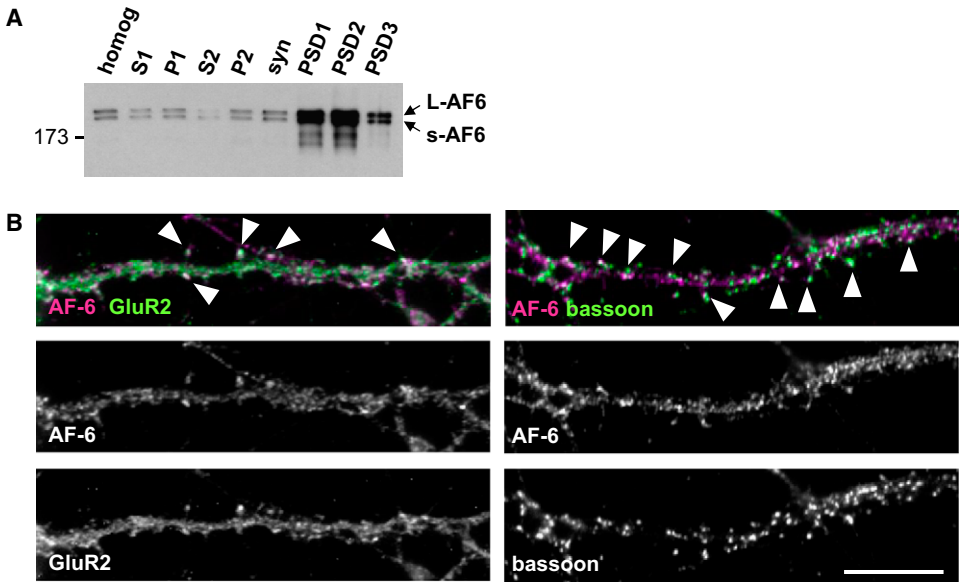

Figure 3. Synaptic Localization of AF-6

(A) Both isoforms of AF-6 are enriched in the postsynaptic density fraction of rat brain. AF-6 is present in both soluble (S1) and particulate (P1) fractions, in roughly equal proportion, and is enriched in synaptosomes (syn) and postsynaptic density fractions (PSD). (B) AF-6 is present at synapses of cultured hippocampal neurons, as shown by partial colocalization with the presynaptic marker bassoon (arrowheads). AF-6 is in a subset of excitatory synapses, as shown by partial colocalization with GluR2 (arrowheads). Scale bar, 10 μm.

activation regulated the subcellular localization and membrane targeting of AF-6; activated Rap1 recruited AF-6 to the plasma membrane, while inactive Rap1 promoted its dissociation from the plasma membrane. We confirmed these results in cortical neurons by overexpressing AF-6 alone or together with Rap1-CA or RapGAP (Figures 4B and 4C). While exogenous AF-6 alone was targeted to both dendritic shafts and spines (Figure 4B, arrowheads), when coexpressed with Rap1-CA, AF-6 was targeted to discrete clusters at the plasma membrane and spine heads (open arrowheads). In contrast, when coexpressed with RapGAP, AF-6 was diffusely distributed inside the dendritic shaft and spine (Figure 4C, inset, arrows). The effects of Rap1 activation on AF-6 localization were quantified by line scanning (Figure 4E). To further analyze the role of Rap1 activation in membrane and synaptic recruitment of AF-6, we generated an N-terminally truncated mutant of AF-6 lacking the two Ras/Rap (RA) binding domains (AF6-ΔN) (Figure 4F). We then examined the effect of Rap1 activation on the subcellular localization of AF6-ΔN (Figures 4D and 4E). Expressed alone, AF6-ΔN was equally distributed between the dendritic shaft and spines. When coexpressed with activated Rap1 (Rap1-CA), AF6-ΔN was diffusely distributed and was not preferentially associated with the plasma membrane or spines. This suggests that binding of activated Rap1 to the RA domains of AF-6 mediates its recruitment to the plasma membrane, while inactivation of Rap1 or deletion of the RA domain of AF-6 leads to a diffuse distribution of AF-6.

AF-6 Regulates Dendritic Spine Morphogenesis

If AF-6 is a mediator of Rap1-regulated structural plasticity, overexpression of AF-6 in neurons should also affect spine morphogenesis. To test this hypothesis, we cotransfected cultures of dissociated cortical neurons (DIV 21) with GFP and the long form of AF-6 (AF-6) (Figure 5). Two days after transfection, exogenous AF-6 was present in dendritic spines (arrowheads) but was also present in a diffuse pattern in the cell body and proximal dendritic shafts, similar to endogenous AF-6 (Figure 5A). Overexpression of AF-6 also induced dramatic spine morphological changes compared to GFP-only controls (area, 1.25 ± 0.98 μm^2 versus 0.47 ± 0.29 μm^2; length, 2.79 ± 1.2 μm versus 1.24 ± 0.5 μm) (Figure 5B), resulting in spines with elongated necks compared to control neurons expressing GFP alone: areas ($p < 0.001$), lengths ($p < 0.001$). These AF-6-induced morphologies closely resembled and were statistically indistinguishable from those induced by activated Rap1 (area, $p = 0.15$; length, $p = 0.44$) or after APV withdrawal (area, $p = 0.86$; length, $p = 0.17$), suggesting a similar mechanism of action. A subset of spines on neurons overexpressing AF-6 had large heads (L on Figure 5A).

We then examined whether the PDZ domain of AF-6 was important in the AF-6 spine targeting and spine morphogenesis by generating a point mutation to abolish its binding to C termini of proteins (AF-6-PDZ*, Figure 4F). When overexpressed in mature neurons, AF-6-PDZ* was targeted to punctate clusters along the dendrites, suggesting that the PDZ domain is not essential for synaptic targeting (Figure 5A). However, neurons expressing AF-6-PDZ* had shorter spines than neurons expressing AF-6 (area, 0.60 ± 0.5 μm^2 versus 1.25 ± 0.98 μm^2, $p < 0.0001$; length, 1.12 ± 0.4 μm versus 2.79 ± 1.2 μm, $p < 0.0001$) and comparable to neurons expressing GFP alone, with a trend toward shorter spines (AF-6-PDZ* versus GFP: area, 0.60 ± 0.5 μm^2 versus 0.47 ± 0.29 μm^2, $p = 0.16$; length, 1.12 ± 0.4 μm versus 1.24 ± 0.5 μm, $p = 0.24$). These results show that AF-6-PDZ* is targeted correctly to dendritic spines but was unable to induce spine morphogenesis.

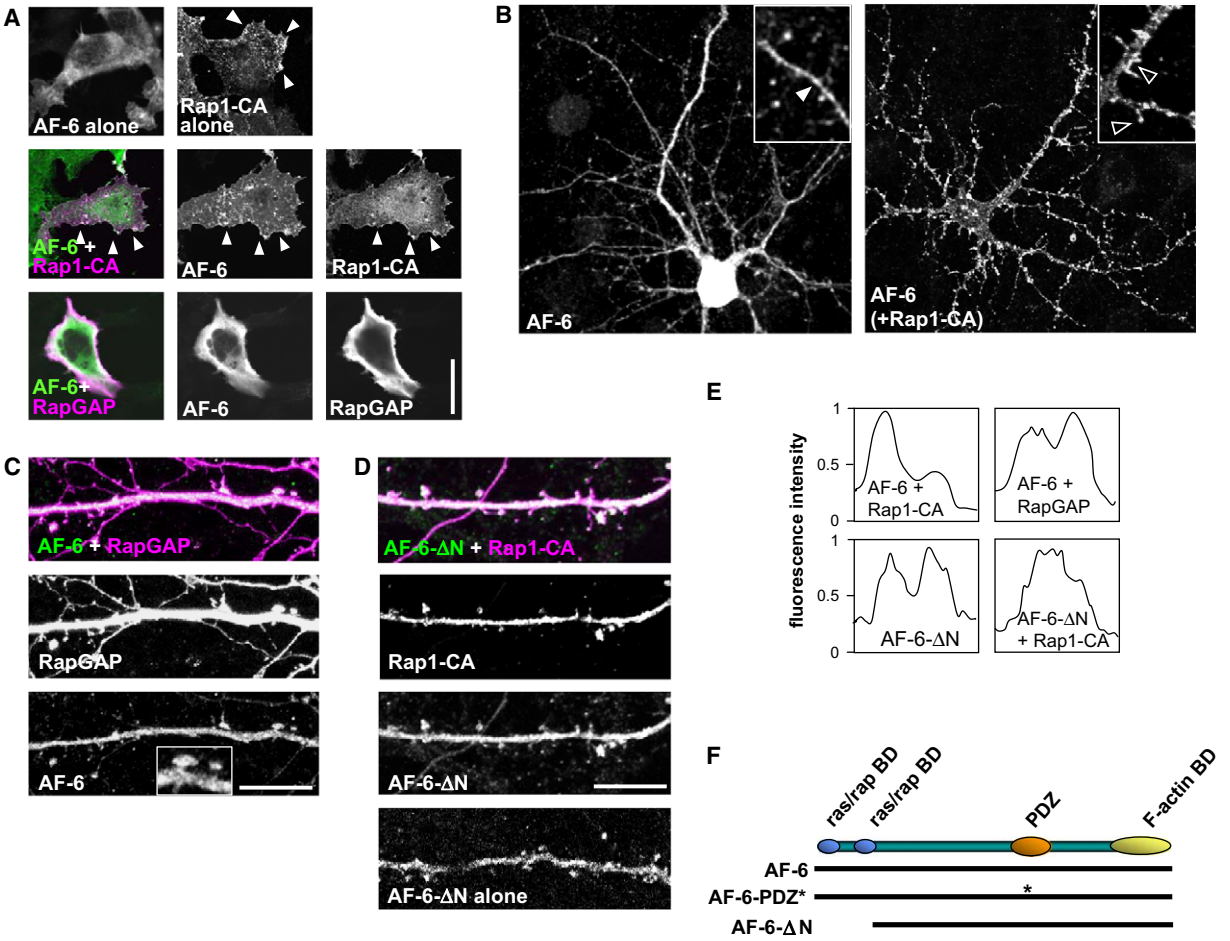

Figure 4. AF-6 Is a Synaptic Target of Rap1

(A) Rap1 activation regulates the subcellular localization of AF-6 in HEK293 cells. HEK293 cells were transfected with *myc*-L-AF-6 or HA-Rap1-CA alone or in combination. AF-6 was also cotransfected with RapGAP1. Forty hours after transfection, cells were fixed and exogenous proteins were detected using antibodies against their tags. Arrowheads show colocalization of AF-6 and Rap1-CA at the plasma membrane. (B) Activated Rap1 (Rap1-CA) induces localization of coexpressed AF-6 to the plasma membrane and spines. While expressed alone in neurons, AF-6 is present in both dendritic shaft and spine heads (left, inset). (C) Inactivation of Rap1 by expression of RapGAP induces spine enlargement and dissociation of AF-6 from the plasma membrane; inset, higher-magnification image of AF-6 containing spines. (D) An N-terminally truncated form of AF-6 lacking the RA domains (AF-6-ΔN), when coexpressed with Rap1-CA, is not associated with the plasma membrane. (E) Quantification of the distribution of AF-6 and AF-6-ΔN alone or in the presence of Rap1 mutants. Normalized fluorescence intensity profiles of AF-6 signals along each spine and dendritic shaft were measured using the "line scan" feature of Metamorph. High-density cultures of cortical neurons (DIV 21) were transfected with *myc*-AF-6 alone or with HA-Rap1-CA, *myc*-Rap1-DN, or flag-RapGAP1 and 40 hr later were fixed and stained; exogenous proteins were detected using combinations of antibodies against the proteins and their tags. (F) Domain structure of AF-6 and constructs used in transfection experiments. The long form of AF-6 contains two ras/rap binding domains (ras/rap BD), a type-II PDZ domain (PDZ) and a filamentous actin-binding domain (F-actin BD). Asterisk indicates the relative position of the point mutation. Scale bar, 10 μm.

To examine the role of the RA domains of AF-6 in regulating spine morphology, we transfected neurons with GFP and AF6-ΔN. Neurons expressing AF6-ΔN had in average larger spines than control neurons (area, 1.52 ± 1.1 versus 0.47 ± 0.29, $p < 0.0001$; length, 1.48 ± 1.1 versus 1.25 ± 0.5, $p < 0.0001$) (Figures 5A and 5B). These results suggest that binding of activated Rap1 to the N-terminal RA domains of AF-6 is required for spine neck elongation.

Rap1-Induced Spine Morphogenesis Is Mediated by the PDZ Domain of AF-6

To test whether AF-6 functioned downstream of Rap1 in regulating spine morphogenesis, we transfected neurons with activated Rap1 (Rap1-CA), together with AF-6-PDZ* and GFP (Figure 5C). Neurons expressing Rap1-CA along with AF-6-PDZ* had smaller spines with reduced spine lengths compared to neurons expressing Rap1-CA alone. This suggests that AF-6-PDZ* interfered with Rap1-induced spine morphogenesis (area, 0.45 ± 0.36 μm^2 versus 1.25 ± 1.08 μm^2, $p < 0.0001$; length, 1.22 ± 0.44 μm versus 2.82 ± 1.6 μm, $p < 0.0001$), reducing it to a phenotype similar to GFP control (area, $p = 0.68$; length, $p = 0.18$) (Figure 5D).

NMDA Receptor Activation-Dependent Translocation of AF-6 into Spines

As we have shown above, activation of NMDA receptors by APV withdrawal activates Rap1, and activated Rap1 recruits AF-6 to the synaptic membrane. These data

suggest that NMDA receptor activation by APV withdrawal may induce translocation of exogenous AF-6. We therefore examined the localization of exogenous *myc*-AF-6 in control and treated neurons (Figure 6A). While in control neurons AF-6 was distributed evenly between spines and the dendritic shaft, in neurons subjected to APV withdrawal AF-6 was almost exclusively present in spines, with a much lower level in shaft (Figure 6A, left). These effects were quantified by line scanning AF-6 immunostaining intensities along a spine and dendritic shaft (Figure 6A, center and right). The differences in ratios of AF-6 staining intensities in spine versus shaft between control and treated neurons were statistically significant by Student's t test (control, 1.6 ± 0.4; APV wd, 3.2 ± 2.1, $p < 0.01$).

Rap1 Inactivation and the AF-6-PDZ* Mutant Block Spine Morphogenesis Induced by APV Withdrawal

To test whether the Rap1/AF-6 pathway mediated structural plasticity induced by NMDA receptor activation, we transfected neurons with RapGAP1 or AF-6-PDZ* along with GFP and subjected them to APV withdrawal (Figure 6B). We observed that APV withdrawal-induced spine morphogenesis was blocked in neurons expressing the mutant proteins. Neurons expressing RapGAP1 and subjected to APV withdrawal had smaller stubby protrusions, without the long necks, compared to neurons expressing only GFP and subjected to APV withdrawal (area, 0.53 ± 0.4 μm^2 versus 1.33 ± 1.0 μm^2, $p < 0.0001$; length, 1.53 ± 0.83 μm versus 2.81 ± 1.53 μm, $p < 0.03$) (Figure 6C). Neurons expressing AF-6-PDZ* and subjected to APV withdrawal had short and stubby spines (area, 0.61 ± 0.45 μm^2 versus 1.33 ± 1.0 μm^2, $p < 0.0002$; length, 1.17 ± 0.56 μm versus 2.81 ± 1.53 μm, $p < 0.0001$). Statistical analysis indicated that the presence of these mutants in neurons reduced the APV withdrawal effect on spine elongation to levels indistinguishable from nontreated control neurons.

Rap1 Regulates AMPA Receptor Content in Spines

Rap1 activation and inactivation resulted in modulation of spine size. Recent studies have suggested that the structure and function of spines are coordinated (Matsuzaki et al., 2001, 2004; Kasai et al., 2003), indicating that spines of different morphologies induced by Rap1 may have different AMPA receptor content. To test this possibility, we examined the effect of activating or inactivating Rap1 on the spine content of GluR1, a subunit of AMPA receptors that is thought to be recruited to synapses during synaptic plasticity (Song and Huganir, 2002; Shi et al., 2001). We therefore transfected cortical neurons with Rap1-CA or RapGAP and examined endogenous GluR1 clusters in spines by immunostaining with an antibody directed against the C terminus of GluR1 (Figure 7). Neurons expressing Rap1-CA had long spines, and GluR1 was present in many but not all spine heads (Figure 7A, white arrows). The size (average area) of the GluR1 clusters in these spine heads was similar to control nontransfected neurons (Figure 7B; Rap1-CA/control ratio = 0.90 ± 0. 14, $p = 0.15$); however, the average total intensity of GluR1 cluster immunostaining was lower in Rap1-CA-expressing neurons (Rap1-CA/control ratio = 0.50 ± 0. 17, $p < 0.001$). The linear density of GluR1 clusters on Rap1-CA-expressing neurons was lower than controls (Rap1-CA, 31.66 ± 8.43 versus control, 47.6 ± 14.2; $p < 0.001$), and some spines had very small GluR1 clusters (Figure 7A, yellow arrowheads). On the other hand, spines on neurons expressing RapGAP were large and contained high levels of GluR1 throughout the spine (Figure 7A, arrowheads), as indicated by the larger average cluster areas, (Figure 7B; RapGAP/control ratio = 1.52 ± 0. 32, $p < 0.001$) and higher intensities of GluR1 clusters (RapGAP/control ratio = 1.51 ± 0. 29, $p < 0.001$). Expression of RapGAP did not affect GluR1 cluster density (Rap1GAP, 46.35 ± 7.59 versus control, 47.6 ± 14.2; $p = 0.87$). Hence Rap1, depending on its activation state, regulates spine size and shape and the AMPA receptor content of spines. AMPA receptor clusters in Rap1-CA induced long spines, as well as in RapGAP-induced large spines were synaptic, as shown by triple staining for GFP-GluR1, the presynaptic marker synaptotagmin, and Rap1 or RapGAP (Figure 7C, open arrowheads).

Discussion

NMDA Receptor-Dependent Spine Structural Plasticity

An increasing body of evidence indicates that structural plasticity, which consists of activity-dependent modifications of synapse size, shape, and number, is a key component of synaptic plasticity during development, adulthood, and disease (Yuste and Bonhoeffer, 2001). However, little is known about the signal transduction mechanisms that regulate structural plasticity. Moreover, although it is becoming clear that structural and functional plasticity of synapses are coordinated, it is unclear how this is achieved at the molecular level (Kasai et al., 2003). Therefore, we set out to identify the key molecular players in the signal transduction mechanisms that regulate structural plasticity. To this end, we developed a method for activity-dependent induction of spine morphogenesis in dissociated cultures of neurons by activating NMDA receptors. Removal of the NMDA receptor blocker APV for a short period of time from neurons cultured in the presence of APV results in activation of presumably synaptic NMDA receptors by spontaneous synaptic activity. This treatment has been previously shown to induce AMPA receptor insertion into silent synapses, potentiation of miniature EPSCs, mobilization of CaMKII into synapses, and AMPA receptor phosphorylation (Liao et al., 1999, 2001). In this study we show that this treatment also results in spine structural plasticity, expressed mainly as spine neck extension. Due to its ability to induce both functional and structural plasticity, this protocol may provide a cell-culture model for spine morphogenesis associated with the induction of plasticity observed in brain slices.

Spine Elongation versus Enlargement

The phenotypes of spine neck elongation or spine head enlargement are intriguing. Both types of spines, thin spines and large spines, exist in the normal rodent and human brain, as shown by serial electron microscopy reconstructions and Golgi studies (Harris et al., 1992; Benavides-Piccione et al., 2002). Similarly, in vivo two-photon imaging of dendrites in mouse barrel and visual cortex revealed that a fraction of spines are thin and

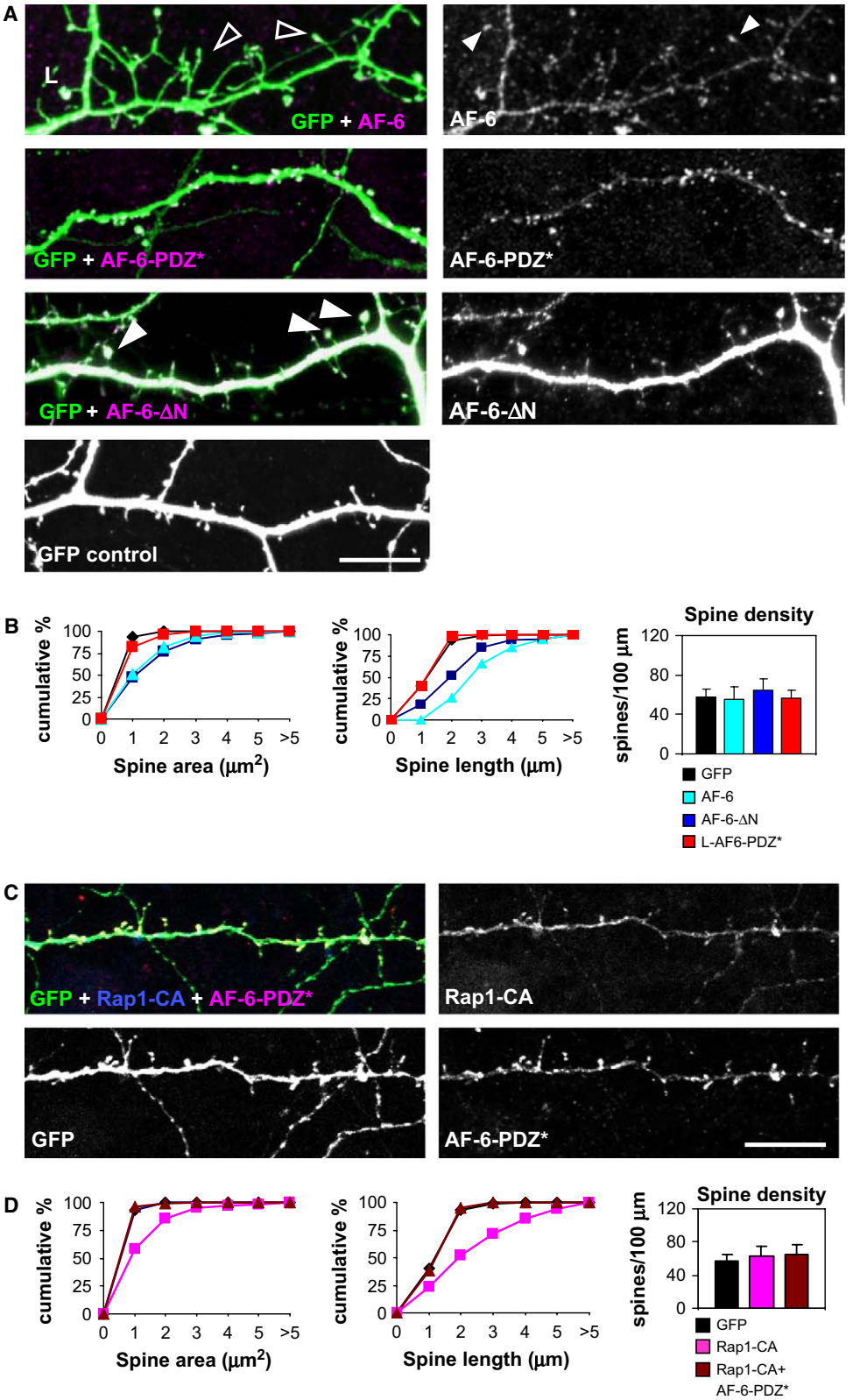

Figure 5. Regulation of Spine Morphogenesis by AF-6

(A) Effects of overexpression of *myc*-tagged AF-6 (long splice variant) PDZ mutant AF-6 (AF6-PDZ*) and AF-6 lacking the RA domains (AF6-ΔN) on spine morphology and spine targeting of the exogenous protein. Arrowheads show localization to spines; L, large spine heads. (B) Quantification of the effects on spine morphogenesis. AF-6 versus GFP-only control: area, (1.25 ± 0.98 μm^2 versus 0.47 ± 0.29 μm^2, $p < 0.0001$); length (2.79 ± 1.2 μm versus 1.24 ± 0.5 μm; $p < 0.0001$). AF-6-PDZ* versus AF-6: area (0.60 ± 0.5 μm^2 versus 1.25 ± 0.98 μm^2, $p < 0.0001$); length (1.12 ± 0.4 μm versus 2.79 ± 1.2 μm, $p < 0.0001$). AF-6-PDZ* versus GFP control: area (0.60 ± 0.5 μm^2 versus 0.47 ± 0.29 μm^2, $p = 0.16$); length (1.12 ±

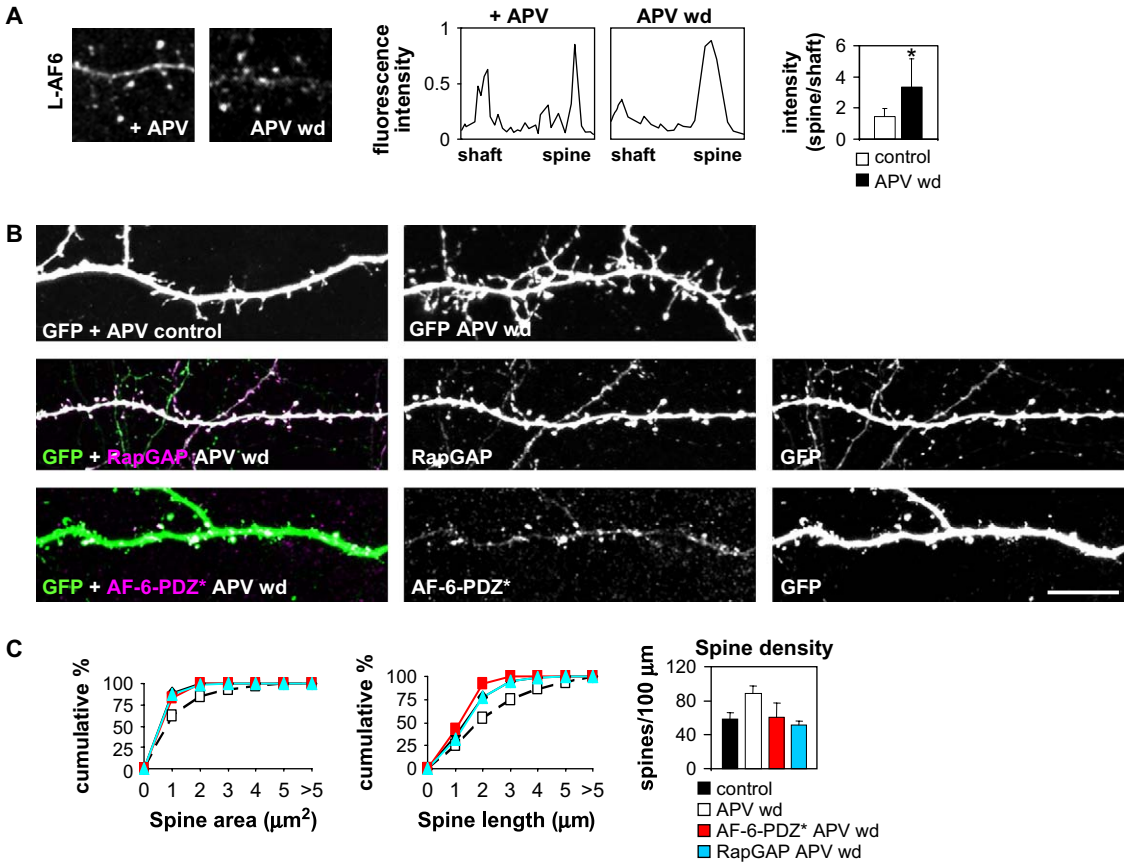

Figure 6. Rap1 and AF-6 Regulate NMDA Receptor Activation-Induced Structural Plasticity of Spines

(A) APV withdrawal induces translocation of exogenous AF-6 from dendritic shafts into spines. Myc-AF-6 was transfected into cortical neurons (DIV 21), and 40 hr later its localization was detected by immunostaining with an anti-*myc* antibody in control neurons and neurons subjected to APV withdrawal (left). Intensity profiles of AF-6 signal along each spine and dendritic shaft were measured using the "line scan" feature of Metamorph (center) and were quantified (right). The differences in ratios of AF-6 staining intensities in spine versus shaft between control and treated neurons were statistically significant by Student's t test (control, 1.6 ± 0.4, APV wd, 3.2 ± 2.1, $p < 0.01$). Bars represent averages of data from three experiments; error bars are standard deviations. (B) Structural plasticity induced by NMDA receptor activation upon APV withdrawal is blocked by inactivation by overexpression of RapGAP1 or AF6-PDZ*. Cortical neurons chronically cultured in the presence of APV (200 μM) were transfected with *myc*-AF-6 alone or GFP alone, or GFP along with flag-RapGAP or *myc*-AF6-PDZ* at DIV 26. Neurons were fixed and immunostained 40 hr later. (C) Quantification of the effects of Rap1 and AF-6-PDZ* on NMDA receptor activation-induced structural plasticity. RapGAP + APV withdrawal versus APV withdrawal control: area (0.53 ± 0.4 μm^2 versus 1.33 ± 1.0 μm^2, $p < 0.0001$), length (1.53 ± 0.83 μm versus 2.81 ± 1.53 μm, $p < 0.03$). AF-6-PDZ* + APV withdrawal versus APV withdrawal control: area (0.61 ± 0.45 μm^2 versus 1.33 ± 1.0 μm^2, $p < 0.0002$), length (1.17 ± 0.56 μm versus 2.81 ± 1.53 μm, $p < 0.0001$). Scale bars, 10 μm. Bars represent averages of data from three experiments; error bars are standard deviations.

long, similar to those induced by NMDA receptor and Rap1 activation and AF-6 overexpression, while another fraction are large with large heads, similar to those induced by Rap1 inactivation and AF-6-ΔN expression (Trachtenberg et al., 2002; Grutzendler et al., 2002; Holtmaat et al., 2005). It is important to clarify that thin spines in the brain and mature neurons are not filopodia, because they contact presynaptic terminals and last for hours to days, while filopodia by definition do not make synapses and last minutes (Trachtenberg et al., 2002; Holtmaat et al., 2005). Similarly, thin spines induced by NMDA receptor and Rap1 activation formed presynaptic contacts (Figures 1C and 7C).

What is the significance of thin spines with elongated necks versus large spines? In vivo imaging studies revealed that thin spines have a much higher turnover rate and are less stable, while the large spines are stable over very long time periods (Trachtenberg et al., 2002; Holtmaat et al., 2005). Such small spines are thought to be highly "plastic," in accordance to their high observed turnover rates and may have a major role in the induction of plasticity, potentially by searching for new

0.4 μm versus 1.24 ± 0.5 μm, $p = 0.24$). AF6-ΔN versus GFP control: area (1.52 ± 1.1 versus 0.47 ± 0.29, $p < 0.0001$); length (1.48 ± 1.1 versus 1.24 ± 0.5, $p < 0.0001$). Bars represent averages of data from three experiments; error bars are standard deviations. (C) AF-6 mediates the spine morphogenic effects of Rap1-CA. Overexpression of AF6-PDZ* blocks Rap1-induced spine morphogenesis. Cortical neurons (DIV 21) were transfected with GFP alone or with *myc*-AF-6, *myc*-AF6-PDZ*, or with *myc*-AF6-PDZ*, and HA-tagged Rap1-CA, and after fixation, GFP was detected using an anti-GFP antibody or by its fluorescence; exogenous AF-6 proteins were detected using an antibody against the *myc* tag. Rap1 expression was detected using a Rap1 antibody. (D) Quantification of the effects on spine morphogenesis. AF-6-PDZ* + Rap1-CA versus Rap1-CA: area (0.45 ± 0.36 μm^2 versus 1.25 ± 1.08 μm^2, $p < 0.0001$); length (1.22 ± 0.44 μm versus 2.82 ± 1.6 μm, $p < 0.0001$). Scale bar, 10 μm. Bars represent averages of data from three experiments; error bars are standard deviations.

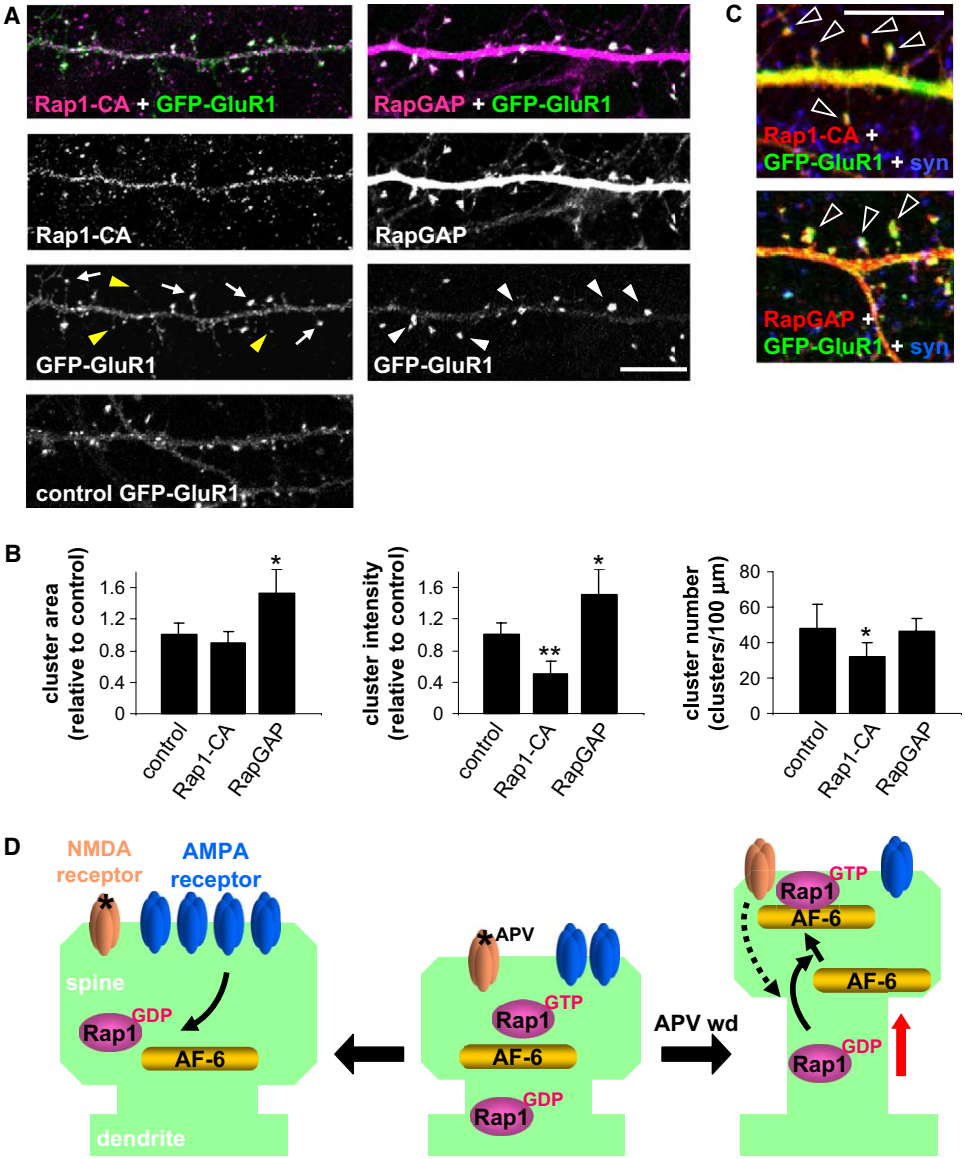

Figure 7. Rap1 Regulates AMPA Receptor Content in Spines

(A) Most thin spines induced by the expression of active Rap1 (Rap1-CA) contain GluR1 clusters (white arrows), while some have very small clusters (yellow arrowheads). Expression of RapGAP induces the formation of large spines with high levels of GluR1 (white arrowheads), compared with nontransfected controls. (B) Quantification of the effects of expression of Rap1 or Rap1GAP on GluR1 cluster area, total fluorescence intensity, and linear density. GluR1 cluster average area (Rap1-CA/control ratio = 0.90 ± 0.14, p = 0.15; RapGAP/control ratio = 1.52 ± 0.32, p < 0.001). GluR1 cluster average total intensity (Rap1-CA/control ratio = 0.50 ± 0.17, p < 0.001; RapGAP/control ratio = 1.51 ± 0. 29, p < 0.001). GluR1 cluster linear density (Rap1-CA, 31.66 ± 8.43 versus control, 47.6 ± 14.2; p < 0.014; Rap1GAP, 46.35 ± 7.59 versus control, 47.6 ± 14.2; p = 0.87). Bars represent averages of data from three experiments; error bars are standard deviations. (C) GluR1 clusters in spine heads induced by Rap1-CA or RapGAP contact presynaptic sites, as revealed by triple staining with antibodies for synaptotagmin (syn), Rap1, or RapGAP, and fluorescence of GFP-GluR1 (arrowheads). Cortical neurons in medium density (DIV 28) were transfected with HA-Rap1 or flag-RapGAP, and after fixation 40 hrs later were stained with antibodies for *myc* or HA and an antibody raised against the C-terminus of GluR1. For synaptic localization, neurons were tranfected with GFP-GluR1 and HA-Rap1 or flag-RapGAP. Scale bars, 10 µm. (D) Model of the regulation of spine structural plasticity and GluR1 content by Rap1 and AF-6. Activation of NMDA receptors by withdrawal of APV results in activation of Rap1. Rap1-GTP binds to the RA motifs of AF-6 and induces its translocation to the postsynaptic plasma membrane, resulting in spine elongation. Inactivation of Rap1 releases AF-6 from the postsynaptic plasma membrane, resulting in spine enlargement and increase in GluR1 content in the spine.

axonal contacts (Kasai et al., 2003; Matsuzaki et al., 2001, 2004). A role in plasticity induction is supported by the observation that similar activity-dependent spine elongation has been observed in several previous studies using different induction protocols and preparations. Formation of thin spines and filopodia was induced in hippocampal neurons by spaced depolarizing stimuli in an NMDA receptor-dependent manner (Wu et al., 2001). Induction of LTP in cultured hippocampal slices resulted in spine neck elongation and formation of new spines with thin long necks (Maletic-Savatic et al., 1999). Similarly, glutamate uncaging in slice cultures resulted in spine elongation (Korkotian and Segal., 1999; Richards et al., 2005). Interestingly, in some of these

experiments the time course of spine elongation was similar to that in our experiments (1–2 hr). Furthermore, activation of CaMKII, a key enzyme downstream of NMDA receptors and essential for plasticity, also induces filopodia growth and spine formation (Jourdain et al., 2003).

Conversely, large spines such as those induced by Rap1 inactivation or AF-6-ΔN expression are hypothesized to be responsible for the maintenance of long-lasting changes in synaptic transmission underlying synaptic plasticity and memory storage (Kasai et al., 2003; Matsuzaki et al., 2001, 2004). This role is further supported by the observed long-term stability of large spines, reported in in vivo imaging studies (Trachtenberg et al., 2002; Grutzendler et al., 2002; Holtmaat et al., 2005). Induction of LTP by high-frequency stimulation or glutamate uncaging resulted in spine head enlargement (Toni et al., 1999; Matsuzaki et al., 2004), suggesting that large spines are also associated with plasticity induction. In fact, it seems that spine enlargement and elongation are both occurring during plasticity, but with different time courses, and different LTP protocols may favor different morphological changes (Korkotian and Segal, 1999; Matsuzaki et al., 2004).

Thin versus large spines may also contribute to plasticity by regulating calcium signaling, because spine necks control the diffusion of calcium between the spine head and dendrite, resulting in chemical compartmentalization of calcium signaling. Long spine necks may slow the calcium diffusion from spine heads, maintaining higher calcium levels and the input specificity, which may be important for the activation and specificity of plasticity signaling mechanisms (Svoboda et al., 1996; Yuste et al., 2000; Korkotian and Segal, 1999; Sabatini et al., 2002; Noguchi et al., 2005).

Interestingly, thin spines reminiscent of those induced by activated Rap1 and AF-6 are characteristic of several types of mental retardation, such as fragile-X syndrome (Purpura, 1974; Fiala et al., 2002; Halpain et al., 2005). It is possible that in these disorders such highly dynamic and unstable spines predominate, resulting in a lack of ability to make stable synaptic contacts, ultimately leading to cognitive impairments.

Molecular Mechanisms of Structural Plasticity

Although many studies reported morphological changes in spines in association with synaptic plasticity induction, the detailed mechanisms by which NMDA receptor activation regulates spine shape remains unknown (Luscher et al., 2000). In this study we identify and characterize such a signaling mechanism, by associating specific morphological changes with specific molecular events. NMDA receptor activation induces spine elongation through Rap1 activation by GTP binding and AF-6 membrane recruitment via binding of activated Rap1 (Figure 7D). In contrast, inactivation of Rap1 and release of AF-6 from the synaptic plasma membrane results in spine enlargement. Although Rap1 signaling has been previously implicated in spine morphogenesis (Pak et al., 2001), our study demonstrates that NMDA receptor activation of Rap1 regulates dendritic spine morphogenesis, and Rap1 functions as a molecular switch to bimodally regulate spine shape. Little is known about the targets of activated Rap1 in general, or in the CNS in particular. Here we identified the PDZ domain-containing protein AF-6 as a postsynaptic target for Rap1 and showed that AF-6 is functionally coupled to NMDA receptor and Rap1 signaling in mediating activity-induced morphological changes in spines. Activation of Rap1 by NMDA receptors results in the binding of GTP-Rap1 to the N-terminal RA domains of AF-6 and its recruitment to the synaptic plasma membrane. Because AF-6 has several protein-protein interaction domains, it may act as a scaffold for the assembly of other signaling molecules at postsynaptic sites. Mutation of the PDZ domain of AF-6 suggests that interactions with downstream partners mediated by this domain may be important in spine morphogenesis. Interestingly, AF-6 interacted in a yeast two-hybrid system with the synaptic Rac1-GEF kalirin-7, a regulator of spine morphogenesis, suggesting that kalirin-7 may mediate the actions of AF-6 on spines (Penzes et al., 2000, 2001). At the synaptic plasma membrane, AF-6 and its associated proteins may induce rearrangements of a specific pool of actin, resulting in spine elongation. Conversely, inactivation of Rap1 results in release of AF-6 from the synaptic plasma membrane, but it doesn't result in its elimination from the spine. Instead, AF-6 is present throughout the spine and thereby may regulate another pool of actin, resulting in spine enlargement.

A recent study concluded that the Rac1-GEF Tiam1 was required for spine structural plasticity induced by an APV withdrawal paradigm similar to the one used in this study (Tolias et al., 2005). Because both pathways are required for spine plasticity, it will be interesting to examine the interaction between the two pathways.

Regulation of AMPA Receptor Content in Spines

Activation of Rap1 induced a decrease in the average intensity and area of GluR1 puncta and resulted in a reduction in the number of GluR1 clusters. Hence, activation of Rap1 is sufficient for reduction of GluR1 content in spines. This reduction was due to the fact that a significant fraction of the thin spines in Rap1-CA-expressing neurons had no or very little GluR1, suggesting that they may be silent synapses. On the other hand, inactivation of Rap1 resulted in a much larger increase in GluR1 content in existing spines, suggesting that Rap1 inactivation is sufficient for AMPA receptor delivery to spines. Our data may reconcile two apparently contradictory studies that implicated Rap1 in LTP and LTD. In the first study, expression of Rap1-CA resulted in depressed AMPA receptor-mediated transmission, while Rap1-DN resulted in potentiation of AMPA receptor-mediated transmission, leading the authors to conclude that Rap1 activity is required for LTD (Zhu et al., 2002). However, another study suggests that inactivation of Rap1 in mouse forebrain impaired cAMP-dependent and theta frequency-induced NMDA receptor-dependent and -independent hippocampal LTP and spatial learning and context discrimination, suggesting a role in late-phase LTP (Morozov et al., 2003). Our results are consistent with these previous studies: NMDA receptor-dependent activation of Rap1 results in spine elongation and formation of potentiatable but not yet potentiated synapses. Hence, the overall the number of AMPA receptor-silent synapse increases, resulting in an apparent synaptic depression. However, synapses on these

thin spines participate in the establishment of late-phase LTP, possibly by allowing formation of new connections; hence, inactivation of Rap1 may result in a shift toward the large spines with high levels of AMPA receptors, which cannot undergo further potentiation, resulting in impaired late-phase LTP and learning.

Two studies by Liao et al. reported that APV withdrawal-induced stimulation of NMDA receptors resulted in AMPA receptor delivery to synapses and potentiation of the mini-EPSCs 20 min after the initiation of APV withdrawal (Liao et al., 1999, 2001). In this study, we examined structural changes in spines at a much later time point following stimulation (2.5 hr after treatment). Several reports found that after stimulation spines undergo multiple stages of structural changes: an initial rapid enlargement (with AMPA receptor insertion) and a later stage of growth of processes and more extensive structural plasticity (Korkotian and Segal, 1999, Matsuzaki et al., 2004; Richards et al., 2005). Hence, it appears that APV withdrawal-induced stimulation of NMDA receptors results in an initial phase of rapid spine delivery of AMPA receptors, as described in Liao et al., 1999, 2001, and a later stage of spine elongation associated with spine neck elongation and decreased GluR1 content in spines. While the initial stage would make synapses stronger, the second stage would make them more plastic.

Coordination of Structural and Functional Plasticity

Morphological and functional changes in synaptic strength are believed to be coordinated; however, the mechanisms by which such coordination is achieved are largely unknown (Luscher et al., 2000; Kasai et al., 2003). Our results indicate that Rap1 and AF-6 coordinate structural and functional plasticity of synapses by regulating spine shape and AMPA receptor content in spines.

What is the significance of coordination between spine shape and AMPA receptor content? Two studies by Matsuzaki et al. reported that thin and small spines, such as those induced by Rap1 activation, have few AMPA receptors and therefore form weak synapses (Matsuzaki et al., 2001, 2004). This is consistent with our findings that activation of Rap1 induces a reduction in the GluR1 content in these thin spines. Such thin and long spines are highly dynamic and may participate in plasticity by the formation of new synapses, as shown during experience-dependent plasticity in the rat barrel cortex (Trachtenberg et al., 2002). Thin spines are potentiatable and may become enlarged and loaded with AMPA receptors and may be responsible for induction of plasticity (Matsuzaki et al., 2001; Kasai et al., 2003). Conversely, large spines such as those induced by Rap1 inactivation or dissociation of AF-6 from the synaptic plasma membrane, are thought to be responsible for maintenance of long-lasting changes in synaptic transmission underlying synaptic plasticity and memory storage (Matsuzaki et al., 2001; Kasai et al., 2003). In the barrel cortex of live mature animals, large spines are much more stable than small spines (Trachtenberg et al., 2002). Thus, Rap1 may act as a molecular switch, which, along with AF-6, coordinates spine shape, dynamics, and the underlying cytoskeleton with AMPA receptor trafficking, and thus regulate synapse stability and efficacy.

Experimental Procedures

Plasmids and Antibodies

HA-Rap1-CA, flag-RapGAP1 plasmids were from Dr. Lawrence Quilliam (Indiana University, Indianapolis, IN); *myc*-Rap1-DN was from Dr. Philip Stork (Vollum Institute, Portland, OR); AF6-*myc* cDNAs were from Dr. Dietmar Vestweber (University of Munster, Germany) and Dr. Kozo Kaibuchi (Nagoya University, Japan). pEGFP-N2 was from Clontech. Rap1 polyclonal antibody was from Upsate Biotechnology, Monoclonal pan-AF-6 antibody was from BD Biosciences and was used at 1:500 for Western blotting, polyclonal pan-AF-6 antibodies were from Drs. Vestweber, Kozo Kaibuchi, and from Sigma and were used at 1:1000 for immunofluorescence and Western blotting. GluR1 C-terminal polyclonal antibody was generated in the Huganir laboratory and was used at 1:400 for immunofluorescence. The AF6-PDZ* mutant was generated by changing Lys 986 in the GLGF motif of the PDZ domain of mouse L-AF-6 into Arg by circular PCR using the following primers: forward, AGAAGCAGAAT GGAATGGGCCGCAGCATTGTTGCAGCAAAGGGT; and reverse, AC CCTTTGCTGCAACAATGCTGCGGCCCATTCCATTCTGCTTCT.

Neuronal Cultures and Transfections

Low-density hippocampal cultures were prepared from rat E18 embryos as described in Liao et al., 2001. Neurons were plated at a density of 0.3×10^6 cells per 60 mm dish onto 18 mm glass coverslips pretreated with poly-L-lysine (1 mg/ml), in plating media (10% horse serum in MEM). After 24 hr, the media was changed to feeding media (Neurobasal media with B27 supplement). Neurons were cultured for 13–21 days before fixation and immunostaining. High-density cortical neuronal cultures were prepared from E18 rat embryos, and neurons were plated onto 18 mm glass coverslips (precoated with poly-L-lysine, 1 mg/ml) or onto 60 mm Petri dishes at a density of 6×10^6 cells per dish, in plating media (10% horse serum in MEM). After 24 hr, cells were placed in feeding media (glia-conditioned 5% horse serum in MEM). Cortical neurons were transfected at DIV 20–25 using Lipofectamine 2000. 2–5 μg of each DNA was mixed with 3 μl of Lipofectamine 2000 in 100 μl of feeding medium were and incubated for 20 min at room temperature. This mixture was added to the cells, which were incubated for 4 hr at 37ºC. Coverslips were then transferred to new medium and kept 48 hr at 37ºC. Hippocampal neurons were transfected at DIV 11 using the same procedure. Neurons were fixed in 3.7% formaldehyde and processed for immunostaining as described (Penzes et al., 2003).

Cell Cultures

HEK293 cells were plated onto glass chamber slides precoated with poly-L-lysine and were cultured in MEM with 10% fetal bovine serum. After 24 hr, cells were transfected using Lipofectamine 2000 reagent (2 μl/well, 2 μg DNA/well). 24 or 48 hr after transfection, cells were processed for immunostaining or harvested for biochemistry.

Neuronal Treatments

Neurons were cultured in the absence or presence of D,L-aminophosphonovalerate (D,L-APV; 200 μM) added to the media 5 days after plating. For treatments, neurons were preincubated in ACSF (125 mM NaCl, 2.5 mM KCl, 26.2 mM $NaHCO_3$, 1 mM NaH_2PO_4, 11 mM glucose, 2.5 mM $CaCl_2$, and 1.25 mM $MgCl_2$) (+ or − APV) for 30 min at 37ºC. Coverslips were then transferred to the treatment chambers in ACSF, following a wash in treatment medium. Neurons were incubated in ACSF without APV plus 100 μM glycine for 30 min, or ACSF with 100 μM glycine for 3 min. After treatment, neurons were used immediately or allowed to recover for 2 hr in ACSF containing pretreatment conditions.

Immunofluorescence Staining

Neurons or HEK293 cells were fixed with 3.7% formaldehyde in PBS containing 10% sucrose for 20 min at room temperature. Cells were permeabilized and blocked simultaneously in a solution containing 10% normal donkey serum, 0.2% Triton X-100 in PBS for 1 hr at room temp. Primary antibodies were added in PBS containing 2% normal donkey serum for 2 hr. After rinsing with PBS four times (30 min total), secondary antibodies were added in PBS containing 2% normal donkey serum. After four rinses (5 min each), coverslips

or slides were mounted using ProLong antifade reagent (Molecular Probes).

Quantitative Analysis of Spine Morphologies

We focused our analysis on cortical pyramidal neurons, as identified by morphology, staining for CaMKII, and lack of staining for GAD65. Transfection efficiencies were variable, between 10-20 cells/coverslip for large constructs and 100 to 200 for small constructs. We included in the analysis all healthy neurons expressing both transfected constructs, at subsaturating expression levels, where targeting could be clearly observed. Neurons with similar expression levels of different proteins were analyzed. Z stacks of images were collected with a Zeiss LSM 510 or Zeiss LSM 5 Pascal confocal microscope using the 63× oil-immersion objective. Reconstructed images generated by compressing the Z stacks were analyzed using the Metamorph (Universal Imaging Corporation) software packages Integrated Morphometry module. Secondary and tertiary dendrites were analyzed. Images were thresholded to exactly outline spines, and area, length, and width were measured for each spine, then the number of spines was divided by the length of the measured dendritic region. Colocalization was analyzed using the "Colocalization" module; images to be compared were taken with the same exposure parameters and thresholded equally. In each experiment, between 400 and 600 spines from 5 to 10 neurons were analyzed per condition. Data were exported into Microsoft Excel for quantitative analysis. Single-factor ANOVA analysis was used to determine the statistical significance of the differences between groups.

Tissue Preparation and Subcellular Fractionation

Rat brain cortex and hippocampal homogenates were prepared by homogenizing tissue in 10 volumes of buffer A: 4 mM HEPES (pH 7.5), 1 mM $MgCl_2$, 0.5 mM $CaCl_2$, and 0.32 M sucrose, containing 0.3 mg/ml PMSF and a protease inhibitor cocktail (LBTI [50 μg/ml], leupeptin [2 μg/ml], benzamidine [16 μg/ml], and pepstatin [2 μg/ml]) using a Teflon homogenizer. Postsynaptic densities were purified using the protocol described in Penzes et al., 2001.

Rap1 Activation Assays

To examine activation of endogenous Rap1 in neurons, we used the "Rap1 activation assay kit" from Upstate Biotechnology. Neurons were harvested in 1 ml lysis buffer (25 mM Tris-HCl [pH 7.4], 250 mM NaCl, 0.5% NP40, 1.25 mM $MgCl_2$, and 5% glycerol) on ice, and positive and negative controls were incubated with 0.1 mM GTPγS and 0.1 mM GDP, respectively, for 20 min at 37ºC. Lysates were cleared by centrifugation at 10 000 × g for 5 min, and supernatants were incubated with 20 μl RBD resin (Rap binding domain of Ral) for 1 hr at 4ºC. The resin pellet was washed three times in 0.5 ml lysis buffer, loaded on SDS-PAGE, and analyzed by Western blotting with the Rap1 polyclonal antibody used at 1:500 dilution (Upstate Biotechnology).

Acknowledgments

We thank Dr. David Linden for critically reading the manuscript; Chun He and Lin Ding for the neuronal cultures; Dr. Lawrence Quilliam (Indiana University, Indianapolis, IN), Dr. Philip Stork (Vollum Institute, Portland, OR), Dr. Dietmar Vestweber (University of Munster, Germany), and Dr. Kozo Kaibuchi (Nagoya University, Japan) for providing valuable plasmids and antibodies. This work was supported by The Howard Hughes Medical Institute and grants from NIMH (1R01MH071316), National Alliance for Autism Research (NAAR), American Federation for Aging Research (AFAR), and National Alliance for Research on Schizophrenia and Depression (NARSAD) for P.P.

Received: July 25, 2005
Revised: September 16, 2005
Accepted: September 28, 2005
Published: November 22, 2005

References

Benavides-Piccione, R., Ballesteros-Yanez, I., DeFelipe, J., and Yuste, R. (2002). Cortical area and species differences in dendritic spine morphology. J. Neurocytol. *31*, 337–346.

Boettner, B., Govek, E.E., Cross, J., and Van Aelst, L. (2000). The junctional multidomain protein AF-6 is a binding partner of the Rap1A GTPase and associates with the actin cytoskeletal regulator profilin. Proc. Natl. Acad. Sci. USA *97*, 9064–9069.

Boettner, B., Harjes, P., Ishimaru, S., Heke, M., Fan, H.Q., Qin, Y., Van Aelst, L., and Gaul, U. (2003). The AF-6 homolog canoe acts as a Rap1 effector during dorsal closure of the Drosophila embryo. Genetics *165*, 159–169.

Buchert, M., Schneider, S., Meskenaite, V., Adams, M.T., Canaani, E., Baechi, T., Moelling, K., and Hovens, C.M. (1999). The junction-associated protein AF-6 interacts and clusters with specific Eph receptor tyrosine kinases at specialized sites of cell-cell contact in the brain. J. Cell Biol. *144*, 361–371.

Caron, E. (2003). Cellular functions of the Rap1 GTP-binding protein: a pattern emerges. J. Cell Sci. *116*, 435–440.

Chen, Y., Wang, P.Y., and Ghosh, A. (2005). Regulation of cortical dendrite development by Rap1 signaling. Mol. Cell. Neurosci. *28*, 215–228.

Chklovskii, D.B., Mel, B.W., and Svoboda, K. (2004). Cortical rewiring and information storage. Nature *431*, 782–788.

Engert, F., and Bonhoeffer, T. (1999). Dendritic spine changes associated with hippocampal long-term synaptic plasticity. Nature *399*, 66–70.

Fiala, J.C., Spacek, J., and Harris, K.M. (2002). Dendritic spine pathology: cause or consequence of neurological disorders? Brain Res. Brain Res. Rev. *39*, 29–54.

Grutzendler, J., Kasthuri, N., and Gan, W.B. (2002). Long-term dendritic spine stability in the adult cortex. Nature *420*, 812–816.

Halpain, S., Spencer, K., and Graber, S. (2005). Dynamics and pathology of dendritic spines. Prog. Brain Res. *147*, 29–37.

Harris, K.M., Jensen, F.E., and Tsao, B. (1992). Three-dimensional structure of dendritic spines and synapses in rat hippocampus (CA1) at postnatal day 15 and adult ages: implications for the maturation of synaptic physiology and long-term potentiation. J. Neurosci. *12*, 2685–2705.

Hering, H., and Sheng, M. (2001). Dendritic spines: structure, dynamics and regulation. Nat. Rev. Neurosci. *2*, 880–888.

Holtmaat, A.J., Trachtenberg, J.T., Wilbrecht, L., Shepherd, G.M., Zhang, X., Knott, G.W., and Svoboda, K. (2005). Transient and persistent dendritic spines in the neocortex in vivo. Neuron *45*, 279–291.

Imamura, Y., Matsumoto, N., Kondo, S., Kitayama, H., and Noda, M. (2003). Possible involvement of Rap1 and Ras in glutamatergic synaptic transmission. Neuroreport *14*, 1203–1207.

Jourdain, P., Fukunaga, K., and Muller, D. (2003). Calcium/calmodulin-dependent protein kinase II contributes to activity-dependent filopodia growth and spine formation. J. Neurosci. *23*, 10645–10649.

Kasai, H., Matsuzaki, M., Noguchi, J., Yasumatsu, N., and Nakahara, H. (2003). Structure-stability-function relationships of dendritic spines. Trends Neurosci. *26*, 360–368.

Korkotian, E., and Segal, M. (1999). Bidirectional regulation of dendritic spine dimensions by glutamate receptors. Neuroreport *10*, 2875–2877.

Kuriyama, M., Harada, N., Kuroda, S., Yamamoto, T., Nakafuku, M., Iwamatsu, A., Yamamoto, D., Prasad, R., Croce, C., Canaani, E., and Kaibuchi, K. (1996). Identification of AF-6 and canoe as putative targets for Ras. J. Biol. Chem. *271*, 607–610.

Lendvai, B., Stern, E.A., Chen, B., and Svoboda, K. (2000). Experience-dependent plasticity of dendritic spines in the developing rat barrel cortex in vivo. Nature *404*, 876–881.

Liao, D., Zhang, X., O'Brien, R., Ehlers, M.D., and Huganir, R.L. (1999). Regulation of morphological postsynaptic silent synapses in developing hippocampal neurons. Nat. Neurosci. *2*, 37–43.

Liao, D., Scannevin, R.H., and Huganir, R. (2001). Activation of silent synapses by rapid activity-dependent synaptic recruitment of AMPA receptors. J. Neurosci. *21*, 6008–6017.

Lin, H., Huganir, R., and Liao, D. (2004). Temporal dynamics of NMDA receptor-induced changes in spine morphology and AMPA receptor recruitment to spines. Biochem. Biophys. Res. Commun. *316*, 501–511.

Linnemann, T., Geyer, M., Jaitner, B.K., Block, C., Kalbitzer, H.R., Wittinghofer, A., and Herrmann, C. (1999). Thermodynamic and kinetic characterization of the interaction between the Ras binding domain of AF6 and members of the Ras subfamily. J. Biol. Chem. *274*, 13556–13562.

Lu, W.Y., Man, H.Y., Ju, W., Trimble, W.S., MacDonald, J.F., and Wang, Y.T. (2001). Activation of synaptic NMDA receptors induces membrane insertion of new AMPA receptors and LTP in cultured hippocampal neurons. Neuron *29*, 243–254.

Luscher, C., Nicoll, R.A., Malenka, R.C., and Muller, D. (2000). Synaptic plasticity and dynamic modulation of the postsynaptic membrane. Nat. Neurosci. *3*, 545–550.

Malenka, R.C., and Nicoll, R.A. (1999). Long-term potentiation—a decade of progress? Science *285*, 1870–1874.

Maletic-Savatic, M., Malinow, R., and Svoboda, K. (1999). Rapid dendritic morphogenesis in CA1 hippocampal dendrites induced by synaptic activity. Science *283*, 1923–1927.

Mandai, K., Nakanishi, H., Satoh, A., Obaishi, H., Wada, M., Nishioka, H., Itoh, M., Mizoguchi, A., Aoki, T., Fujimoto, T., et al. (1997). Afadin: A novel actin filament-binding protein with one PDZ domain localized at cadherin-based cell-to-cell adherens junction. J. Cell Biol. *139*, 517–528.

Mataga, N., Mizuguchi, Y., and Hensch, T.K. (2004). Experience-dependent pruning of dendritic spines in visual cortex by tissue plasminogen activator. Neuron *44*, 1031–1041.

Matsuzaki, M., Ellis-Davies, G.C., Nemoto, T., Miyashita, Y., Iino, M., and Kasai, H. (2001). Dendritic spine geometry is critical for AMPA receptor expression in hippocampal CA1 pyramidal neurons. Nat. Neurosci. *4*, 1086–1092.

Matsuzaki, M., Honkura, N., Ellis-Davies, G.C., and Kasai, H. (2004). Structural basis of long-term potentiation in single dendritic spines. Nature *429*, 761–766.

Mizoguchi, A., Kim, S., Ueda, T., Kikuchi, A., Yorifuji, H., Hirokawa, N., and Takai, Y. (1990). Localization and subcellular distribution of smg p25A, a ras p21-like GTP-binding protein, in rat brain. J. Biol. Chem. *265*, 11872–11879.

Morozov, A., Muzzio, I.A., Bourtchouladze, R., Van-Strien, N., Lapidus, K., Yin, D., Winder, D.G., Adams, J.P., Sweatt, J.D., and Kandel, E.R. (2003). Rap1 couples cAMP signaling to a distinct pool of p42/44MAPK regulating excitability, synaptic plasticity, learning, and memory. Neuron *39*, 309–325.

Nagerl, U.V., Eberhorn, N., Cambridge, S.B., and Bonhoeffer, T. (2004). Bidirectional activity-dependent morphological plasticity in hippocampal neurons. Neuron *44*, 759–767.

Noguchi, J., Matsuzaki, M., Ellis-Davies, G.C., and Kasai, H. (2005). Spine-neck geometry determines NMDA receptor-dependent Ca2+ signaling in dendrites. Neuron *46*, 609–622.

Nishioka, H., Mizoguchi, A., Nakanishi, H., Mandai, K., Takahashi, K., Kimura, K., Satoh-Moriya, A., and Takai, Y. (2000). Localization of l-afadin at puncta adhaerentia-like junctions between the mossy fiber terminals and the dendritic trunks of pyramidal cells in the adult mouse hippocampus. J. Comp. Neurol. *424*, 297–306.

Oray, S., Majewska, A., and Sur, M. (2004). Dendritic spine dynamics are regulated by monocular deprivation and extracellular matrix degradation. Neuron *44*, 1021–1030.

Pak, D.T., Yang, S., Rudolph-Correia, S., Kim, E., and Sheng, M. (2001). Regulation of dendritic spine morphology by SPAR, a PSD-95-associated RapGAP. Neuron *31*, 289–303.

Penzes, P., Johnson, R.C., Alam, M.R., Kambampati, V., Mains, R.E., and Eipper, B.A. (2000). An isoform of kalirin, a brain-specific GDP/GTP exchange factor, is enriched in the postsynaptic density fraction. J. Biol. Chem. *275*, 6395–6403.

Penzes, P., Johnson, R.C., Sattler, R., Zhang, X., Huganir, R.L., Kambampati, V., Mains, R.E., and Eipper, B.A. (2001). The neuronal Rho-GEF Kalirin-7 interacts with PDZ domain-containing proteins and regulates dendritic morphogenesis. Neuron *29*, 229–242.

Penzes, P., Beeser, A., Chernoff, J., Schiller, M.R., Eipper, B.A., Mains, R.E., and Huganir, R.L. (2003). Rapid induction of dendritic spine morphogenesis by trans-synaptic ephrinB-EphB receptor activation of the Rho-GEF Kalirin. Neuron *37*, 263–274.

Purpura, D.P. (1974). Dendritic spine "dysgenesis" and mental retardation. Science *186*, 1126–1128.

Rebhun, J.F., Castro, A.F., and Quilliam, L.A. (2000). Identification of guanine nucleotide exchange factors (GEFs) for the Rap1 GTPase: regulation of MR-GEF by M-Ras-GTP interaction. J. Biol. Chem. *275*, 34901–34907.

Richards, D.A., Mateos, J.M., Hugel, S., de Paola, V., Caroni, P., Gahwiler, B.H., and McKinney, R.A. (2005). Glutamate induces the rapid formation of spine head protrusions in hippocampal slice cultures. Proc. Natl. Acad. Sci. USA *102*, 6166–6171.

Rubinfeld, B., Munemitsu, S., Clark, R., Conroy, L., Watt, K., Crosier, W.J., McCormick, F., and Polakis, P. (1991). Molecular cloning of a GTPase activating protein specific for the Krev-1 protein p21rap1. Cell *65*, 1033–1042.

Sabatini, B.L., Oertner, T.G., and Svoboda, K. (2002). The life cycle of Ca(2+) ions in dendritic spines. Neuron *33*, 439–452.

Shi, S., Hayashi, Y., Esteban, J.A., and Malinow, R. (2001). Subunit-specific rules governing AMPA receptor trafficking to synapses in hippocampal pyramidal neurons. Cell *105*, 331–343.

Sheng, M., and Kim, M.J. (2002). Postsynaptic signaling and plasticity mechanisms. Science *298*, 776–780.

Song, I., and Huganir, R.L. (2002). Regulation of AMPA receptors during synaptic plasticity. Trends Neurosci. *25*, 578–588.

Stork, P.J. (2003). Does Rap1 deserve a bad Rap? Trends Biochem. Sci. *28*, 267–275.

Svoboda, K., Tank, D.W., and Denk, W. (1996). Direct measurement of coupling between dendritic spines and shafts. Science *272*, 716–719.

Tolias, K.F., Bikoff, J.B., Burette, A., Paradis, S., Harrar, D., Tavazoie, S., Weinberg, R.J., and Greenberg, M.E. (2005). The Rac1-GEF Tiam1 couples the NMDA receptor to the activity-dependent development of dendritic arbors and spines. Neuron *17*, 525–538.

Toni, N., Buchs, P.A., Nikonenko, I., Bron, C.R., and Muller, D. (1999). LTP promotes formation of multiple spine synapses between a single axon terminal and a dendrite. Nature *402*, 421–425.

Trachtenberg, J.T., Chen, B.E., Knott, G.W., Feng, G., Sanes, J.R., Welker, E., and Svoboda, K. (2002). Long-term in vivo imaging of experience-dependent synaptic plasticity in adult cortex. Nature *420*, 788–794.

Wong, W.T., and Wong, R.O. (2000). Rapid dendritic movements during synapse formation and rearrangement. Curr. Opin. Neurobiol. *10*, 118–124.

Wong, W.T., Faulkner-Jones, B.E., Sanes, J.R., and Wong, R.O. (2000). Rapid dendritic remodeling in the developing retina: dependence on neurotransmission and reciprocal regulation by Rac and Rho. J. Neurosci. *20*, 5024–5036.

Wu, G.Y., Deisseroth, K., and Tsien, R.W. (2001). Spaced stimuli stabilize MAPK pathway activation and its effects on dendritic morphology. Nat. Neurosci. *4*, 151–158.

Yuste, R., and Bonhoeffer, T. (2001). Morphological changes in dendritic spines associated with long-term synaptic plasticity. Annu. Rev. Neurosci. *24*, 1071–1089.

Yuste, R., Majewska, A., and Holthoff, K. (2000). From form to function: calcium compartmentalization in dendritic spines. Nat. Neurosci. *3*, 653–659.

Zhu, J.J., Qin, Y., Zhao, M., Van Aelst, L., and Malinow, R. (2002). Ras and Rap control AMPA receptor trafficking during synaptic plasticity. Cell *110*, 443–455.